JMEPEG (2013) 22:2623–2633
DOI: 10.1007/s11665-013-0540-0

1059-9495/$19.00

Effect of Gas Composition on Nitriding and Wear Behavior of Nitrided Titanium Alloy Ti-15V-3Cr-3Al-3Sn

C. Anandan, P.Dilli Babu, and L. Mohan

(Submitted November 8, 2012; in revised form December 26, 2012; published online April 6, 2013)

Titanium alloy, Ti-15V-3Cr-3Al-3Sn was nitrided at different temperatures with low pressure plasma with 100% nitrogen, and nitrogen diluted with hydrogen and argon. The nitrided layers were characterized for hardness, structure, and composition. Nitrided samples show weight gain that depended on temperature and duration of nitriding. EDS results show that intake of nitrogen is significant at temperatures above 750 °C. Hydrogen dilution increases intake of nitrogen. Samples nitrided with hydrogen dilution have lower surface roughness and higher nitrogen concentration. Depth profiling by XPS shows the formation of nitride in the near-surface region and also that nitrogen concentration in the interior of the nitrided layers is higher at higher temperatures. Micro Raman shows that formation of nitride takes place at higher temperatures. XRD shows that the nitrided layers consist predominantly of alpha Ti and Ti_2N. This is reflected in the hardness increase and hardness profile in the nitrided samples. The low intake of nitrogen by the alloy is attributed to the low solubility of nitrogen in beta alloy and low diffusion coefficient of nitrogen. Reciprocating wear studies showed a lower coefficient of friction and lower wear loss for nitrided samples compared to that of substrate.

Keywords gas dilution, hardness, plasma nitriding, Ti-15-3, titanium alloy, wear, XPS

1. Introduction

Titanium and its alloys have high strength-to-weight ratio and possess excellent corrosion resistance. Pure Titanium is an α alloy, and the α-to-β transformation occurs at about 885 °C. Depending on the nature of alloying elements and their concentration, titanium alloys can exist in α, β, or α + β form, and the transformation temperature may be higher or lower than pure titanium (Ref 1). In case of α + β alloy, Ti-6Al-4V, the α-to-β transformation occurs at 980 °C. On the other hand, beta alloys are a class of alloys for which the transus temperature can be as low as 750 °C (Ref 1, 2). Most of the metal-forming operations of the titanium alloys are performed at high temperatures because of the high temperatures needed for inducing plastic flow. However, these high temperatures are energy intensive. Also these thermomechanical treatments may induce unwarranted metallurgical changes in the base material. The low beta transus temperature of titanium alloys make them amenable to lower-temperature operations compared with α + β alloys. Among the several β alloys, vanadium-containing alloys such as Ti-10-2-3 and Ti-15-3—find prominent place in aerospace sector. For example, Ti-10-2-3 has been used in landing gear application in aircraft and Ti-15-3 has found several applications in aerospace industry (Ref 2).

C. Anandan, P. Dilli Babu, and **L. Mohan**, Surface Engineering Division, CSIR—National Aerospace Laboratories, P.O. Box 1779, Old Airport Road, Bangalore 560 017 Karnataka, India. Contact e-mail: canandan@nal.res.in.

While titanium alloys possess high strength-to-weight ratio and good corrosion resistance, they suffer from poor wear resistance. They are prone to severe galling and scouring in the presence of moving contacts (Ref 3, 4). Therefore, usage of titanium alloys is mainly restricted to components under static loading conditions in many industries, mainly in aerospace and chemical industries (Ref 2, 3, 5). For applications that require wear resistance, therefore, it is necessary to increase the surface hardness of these alloys (Ref 5-7). Surface modifications by ion implantation, (Ref 4, 8-11) nitriding, (Ref 11-13), and duplex treatments (Ref 6, 7) have been carried out on titanium alloys. The nitriding behaviors of pure titanium and the most popular titanium alloy Ti-6Al-4V have been well documented (Ref 11, 14-17). These studies show that effective nitriding takes place at temperatures close to the beta transus temperatures. Since the beta transus temperature of beta alloys is low, it is expected that effective nitriding of these alloys can be carried out at lower temperatures. However, in the case of beta alloys, only limited reports are available on their nitriding behavior. Of these, the study by Zhecheva et al. is notable (Ref 18-20). Those experiments were carried out in gas phase in the temperature range of 800-1050 °C and at pressures of few Pascals. Their main observation has been that the extent to which beta alloys can be nitrided is limited. For example, their investigations of Ti-10-2-3 and LCB have shown that the nitride-layer thicknesses in these alloy are low, and hardness increase is also low (Ref 20).

The present article reports the results of a detailed investigation on nitriding of the beta alloy Ti-15V-3Cr-3Al-3Sn (Ti-15-3)—in a low-pressure nitrogen plasma in the temperature range of 600-900 °C instead of gas nitriding. The results show that the alloy's nitridability is low and higher temperatures, i.e., >800 °C, as in the case of Ti-6Al-4V, are needed to effectively nitride these alloys. Also, effects of hydrogen and argon dilution of nitrogen on nitriding of the alloy are discussed.

2. Materials and Methods

Titanium alloy, Ti-15-3, was procured in the form of 2-mm-thick sheets from M/s. Titanium Metal Corporation, USA. The composition of the material is 15V, 2.98Cr, 3.12Al, 3.05Sn, 0.15Fe and the balance Ti. The beta transus temperature is in the range of 750-775 °C. Flat samples of dimensions $25 \times 25 \times 2$ mm^3, size were used for nitriding experiments. These samples were prepared for plasma nitriding by grinding with silicon carbide sheets of grit sizes varying from 400 to 1200 and polished with 0.3 μm alumina. Finally, they were ultrasonically cleaned with acetone for 10 minutes and weighed using a Sartorius balance before loading into the vacuum chamber. The roughness of the samples after polishing was 0.07 μm. The vacuum chamber was evacuated to a pressure of less than 4×10^{-6} mbar, and the samples were heated to the required temperature on a heating stage. Plasma nitriding was carried out at 600, 700, 750, 800, 850, and 900 °C with atmospheres of 100% N, 80% N-20% H, and 80% N-20% Ar. Plasma was generated using 13.56-MHz RF generator at 50 W. The details of the temperature and duration of the experiments are given in Table 1. After nitriding, the samples were cooled to room temperature under vacuum and analyzed for change in weight, roughness, hardness, and composition.

Table 1 Plasma-nitriding temperatures and durations for different gas compositions

	Duration in hours		
Temperature (°C)	100% N	80:20 (N:H)	80:20 (N:Ar)
700	4	4	…
700	8	8	…
750	4	4	…
750	8	8	…
800	4	4	4
800	8	8	8
850	4	4	…
850	8	8	…
900	8	4	…

The nitrided samples were weighed after treatment. The surface hardness values of the nitrided samples were measured using the Buehler® Micromet Testing Machine with Knoops' indenter at loads of 25, 50, 100, and 200 gf. The substrate hardness is in the range of 350-360 HK at 50-gf load. The cross-sectional hardness profile of the samples was measured at 50-gf load after molding them in resin mould and polishing. The cross-sectional optical micrographs of the nitrided edge were obtained after etching the polished samples using Kroll's reagent (25 mL H_2O + 2 mL conc. HNO_3 + 1 mL conc. HF) for 15 s. The roughness of the samples was measured using Mitutoyo surface profiler. The presence of various phases in the nitrided layer was identified by means of X-Ray diffraction (XRD) using PHILIPS X-ray diffractometer (BRUKER, Germany). A monochromatic source, Cu K_α radiation (λ = 0.1548 nm), was used,

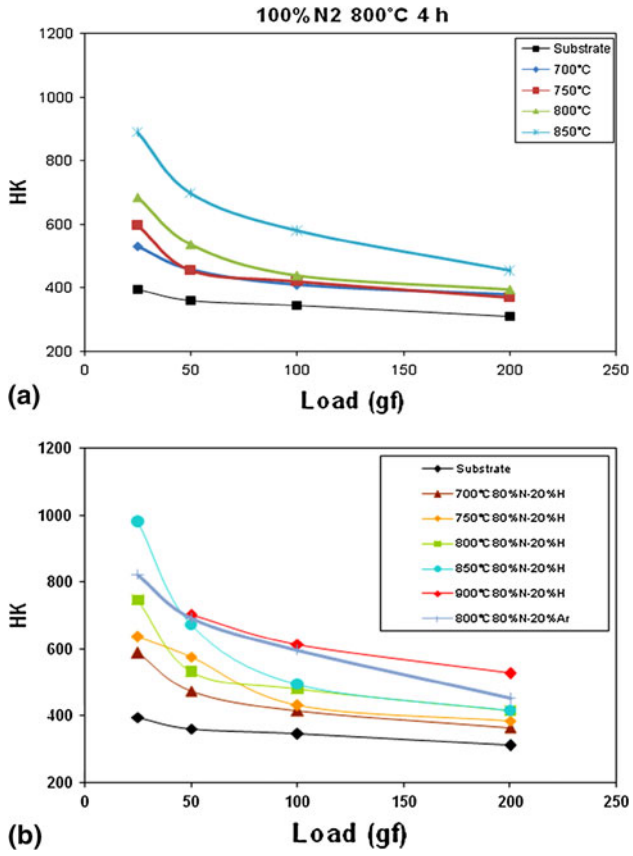

Fig. 1 Surface Hardness of samples nitrided for 4 h at different temperatures with different gas compositions: (a) 100% nitrogen, (b) 20% hydrogen-diluted nitrogen and argon-diluted nitrogen

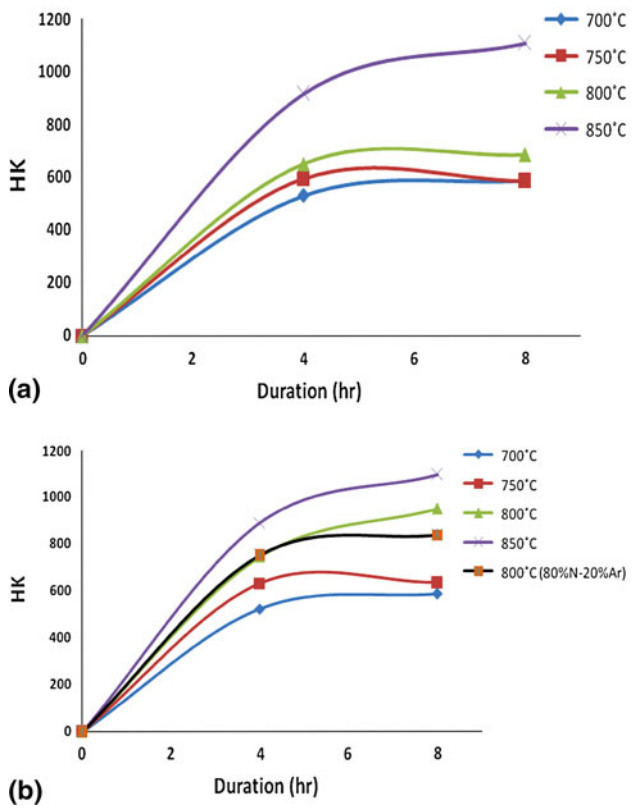

Fig. 2 Variation of hardness with nitriding time for different gas compositions: (a) 100% N and (b) 80% N-20% H and 80% N-20% Ar

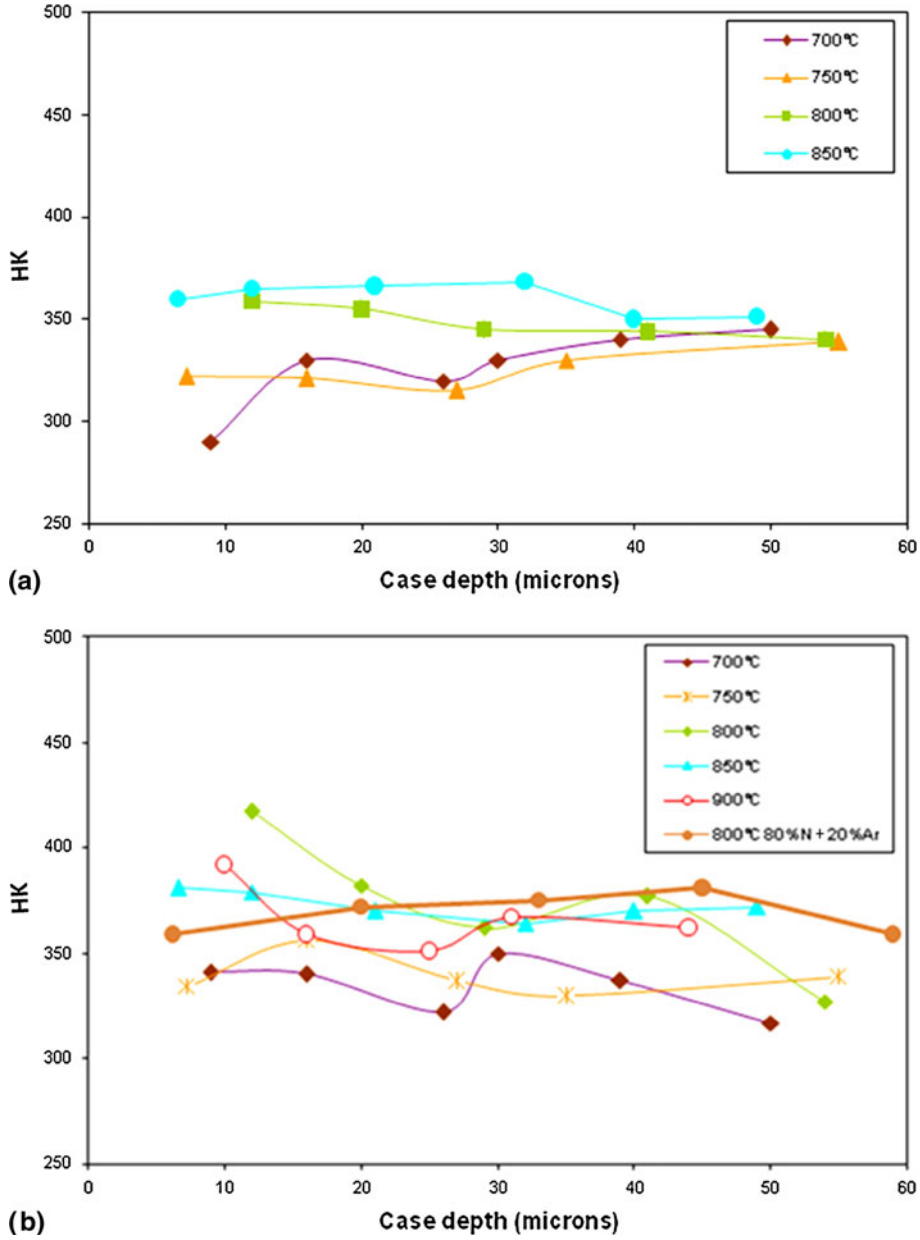

Fig. 3 Cross-sectional hardness for samples nitrided at different temperature and gas compositions: (a) 100% N and (b) 80% N-20% H and 80% N-20% Ar

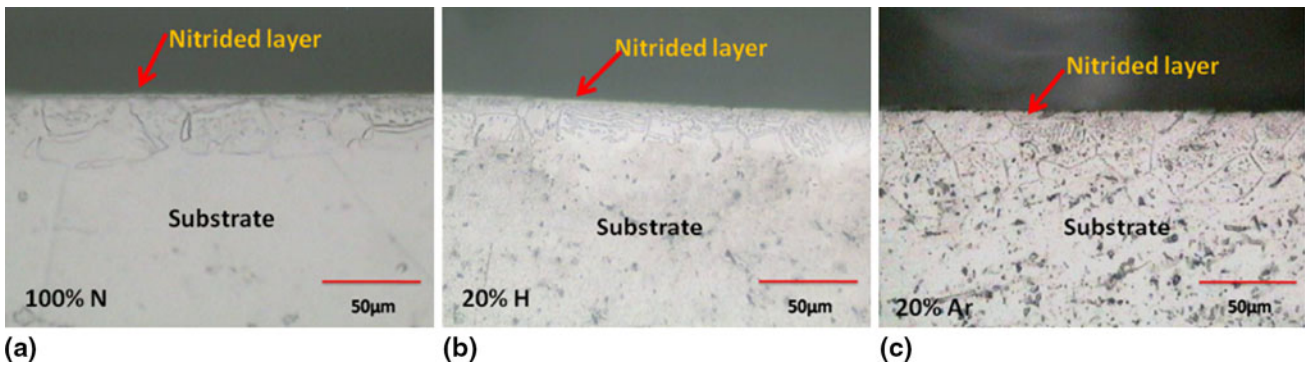

Fig. 4 Cross-sectional optical micrographs of samples nitrided at different gas compositions: (a) 8 h/800 °C in 100% N, (b) 4 h/800 °C in 80% N-20% H, and (c) 4 h/800 °C in 80% N-20% Ar (500×)

and the samples were scanned from 0° to 80° at a scanning rate of 0.5°/min. Micro Raman spectra were obtained using Labram 010 Model of DILOR-JOBIN-YVON-SPEX Micro Raman spectrometer with 623.4-nm laser. The surface morphologies of the samples were examined through Carl Zeiss Supra 40 VP FESEM. The composition of the nitrided layer was obtained using Inca Penta Fetx3 (Oxford) EDAX analyzer attached to the FESEM and also by means of X-ray Photoelectron Spectroscopy (XPS). The XPS spectra were obtained on a SPECS XPS system equipped with a hemispherical analyzer and a single-channel detector, and twin anode X-ray source. Core level spectra of Ti2p and N1s were obtained using 100-W Al K_α radiation at a pass energy of 25 eV. The spectra were obtained in the as-received condition, and after sputter etching with argon ions. Elemental distribution in the nitrided layer was obtained by sputter profiling using 1 keV argon ions at a pressure of 1×10^{-5} mbar and recording the spectra after each sputtering. Wear studies were carried out on a reciprocating-type wear tester (Model CM 9084 DuCom) (Ref 21). An alumina ball of 6-mm diameter was used as the counter surface. A stroke length of 10 mm and a frequency of 100 Hz/min were used at 3 and 5N normal forces. The duration of experiment was 20 min. After

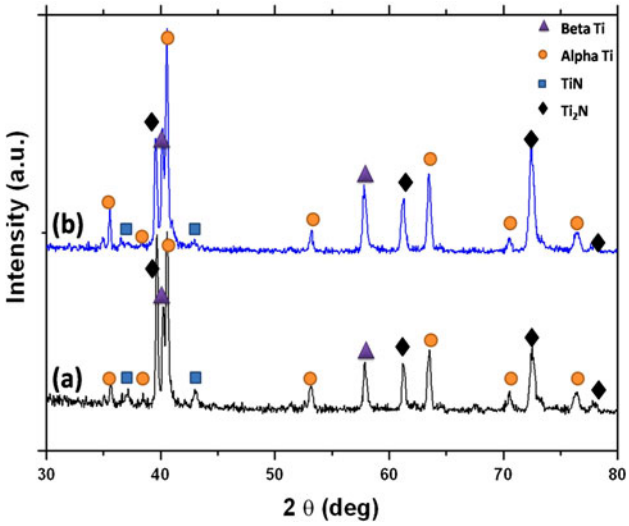

Fig. 5 X-ray diffraction pattern for (a) sample nitride at 850 °C for 4 h in 100% nitrogen, and (b) sample nitride at 800 °C for 4 h in hydrogen-diluted nitrogen

Table 2 Nitrogen concentration in at.% in samples nitrided in 100% N for 8 h

Temperature (°C)	600	700	750	800	850
N (at.%)	2.56	12.99	17.92	18.13	33.77

Table 3 Comparison of N at.% after nitriding for 8 h with different gas compositions

Temperature (°C)	Gas composition	N (at.%)
750	100% N	17.92
750	80% N-20% H	20.25
800	100% N	18.13
800	80% N-20% H	24.26
800	80% N-20% Ar	17.68

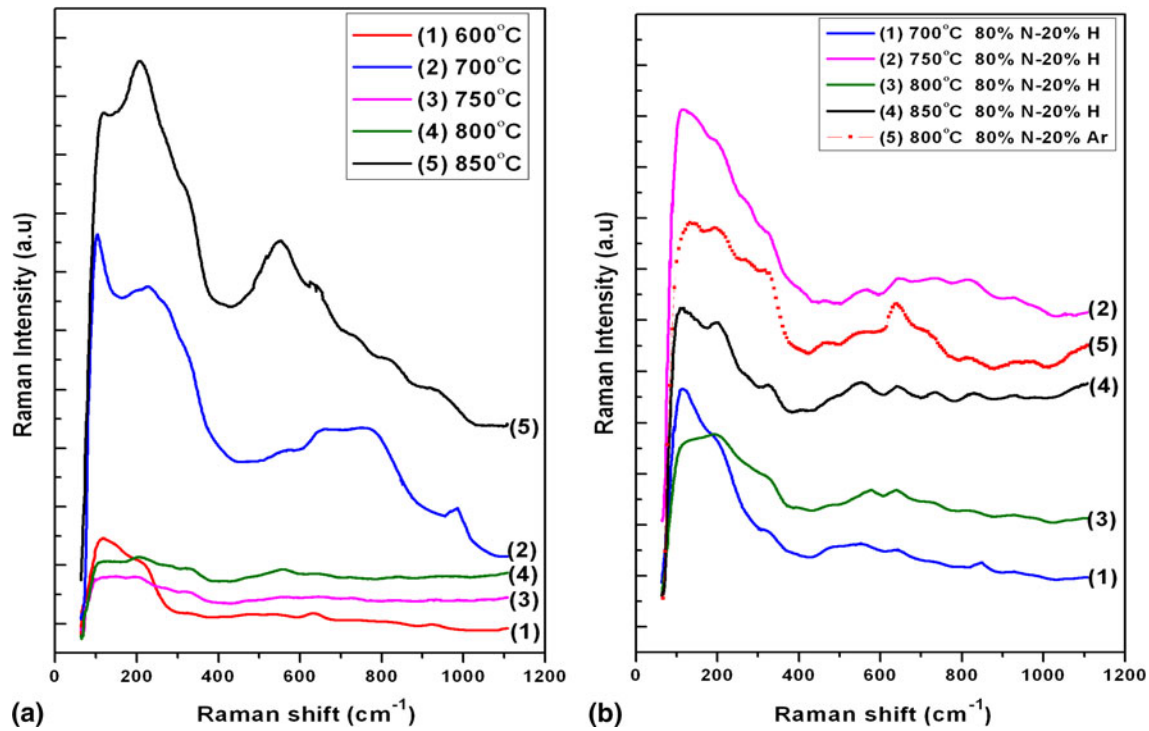

Fig. 6 Raman spectra of samples treated at different temperatures for 8 h (a) 100% N and (b) 80% N-20% H and 80% N-20% Ar

the experiments, the samples were examined for wear profile using 2D and 3D profilometer, Nanomap 500 LS.

3. Results and Discussion

The roughness of the substrate before nitriding was 0.07 μm. The roughness increased marginally to about 0.08 μm after nitriding in 100% nitrogen, especially at higher temperatures. After nitriding with hydrogen dilution, the roughness was 0.05 μm. There was marginal effect of temperature in this case. With argon dilution, the roughness increased slightly to 0.09 μm. With increasing duration of nitriding, the roughness also increased in this case. All the nitrided samples showed a weight gain. The weight gain depended on the nitriding temperature, duration and gas composition. Significant weight gain was observed only after nitriding at greater than 750 °C. Dilution of nitrogen with hydrogen seems to increase nitrogen intake by the sample.

The surface hardness of samples nitrided at different temperatures for 4 h in 100% nitrogen and nitrogen diluted with 20% hydrogen and 20% argon, are shown in Fig. 1(a) and (b), respectively. It can be observed from the figures that the hardness of the samples increases with temperature. The hardness at 25 gf has increased by 2-3 times after nitriding at higher temperatures. A comparison of the graphs shows that increase in hardness is higher after nitriding with hydrogen-diluted nitrogen compared with nitriding in 100% nitrogen- or Ar-diluted nitrogen. Also, the decrease of hardness with load is less steep in this case. Figure 2(a) and (b) shows the dependence of hardness on nitriding duration at different temperatures. The graphs show that the hardness increases with time, but significant increase is again found only after nitriding at greater than 750 °C.

Hardness profiles are shown in Fig. 3(a) and (b) for samples nitrided at different temperatures with different gas compositions. The data were obtained at a load of 50 gf. As can be seen in the graphs, hardness has not increased in the subsurface region of the nitrided layers. The expected trend of a high hardness at the surface that decreases with depth into the substrate is not observed. The hardness remains almost constant. Similar observations have been made by Sha and Malinov (Ref 20) and Zhecheva et al. (Ref 17, 18) in their gas-nitriding experiments on beta titanium alloys. Samples treated under 80% N-20% H show a comparatively higher hardness up to about 20 μm.

Optical micrographs of the cross section of the sample nitrided at 800 °C for 8 h using 100% nitrogen and samples nitrided at 800 °C for 4 h using hydrogen- and argon- diluted nitrogen are given in Fig. 4(a)-(c), respectively. Very thin nitrided layers can be seen in the figures, implying very thin nitride-layer formation along with α-phase in the near-surface region. The thin nitrided edge shows that the alloy is difficult to nitride. This is further discussed later.

X-ray diffraction patterns from the samples nitrided at 850 °C using 100% N and at 800 °C using hydrogen diluted nitrogen are given in Fig. 5(a) and (b). The location of different peaks pertaining to (β) beta phase, (α) alpha phase, and nitrides, TiN and Ti_2N, are shown in the figures (Ref 20, 22, 23). After nitriding, appearance of α phase can be seen along with the nitrides. The intensity of the TiN phase is much lower than that of Ti_2N. This shows that predominantly Ti_2N is formed along with alpha-phase formation. In the sample nitrided with hydrogen dilution, the intensities of the alpha and Ti_2N peaks are higher implying greater intake of nitrogen.

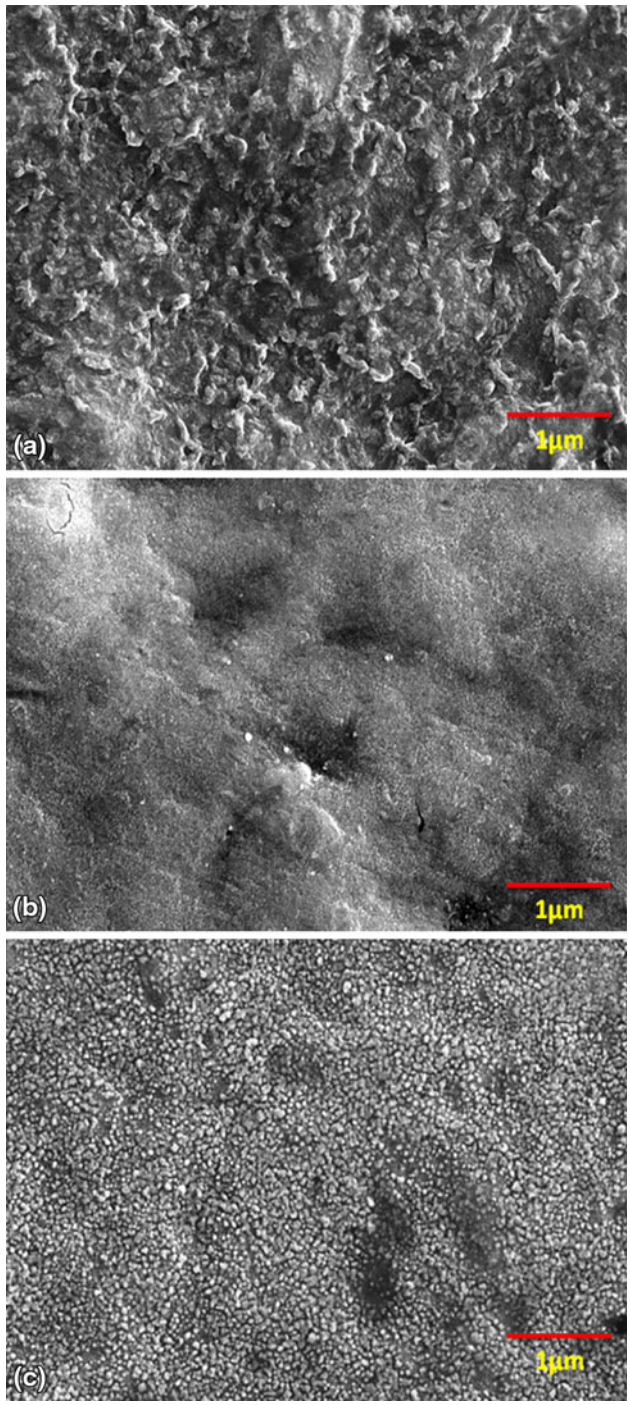

Fig. 7 FESEM images of samples nitride for 8 h at 800 °C: (a) 100% N, (b) 80% N-20% H, and (c) 80% N-20% Ar

Figure 6(a) and (b) shows the micro Raman spectra of samples nitrided at different temperatures using 100% nitrogen and 20% hydrogen- and argon-diluted cases. For TiNx, the transverse optical and longitudinal optical (TO + LO) phonon peaks occur in the 500-800 cm^{-1} wave number range, which correspond to titanium vacancies in the lattice. The transverse

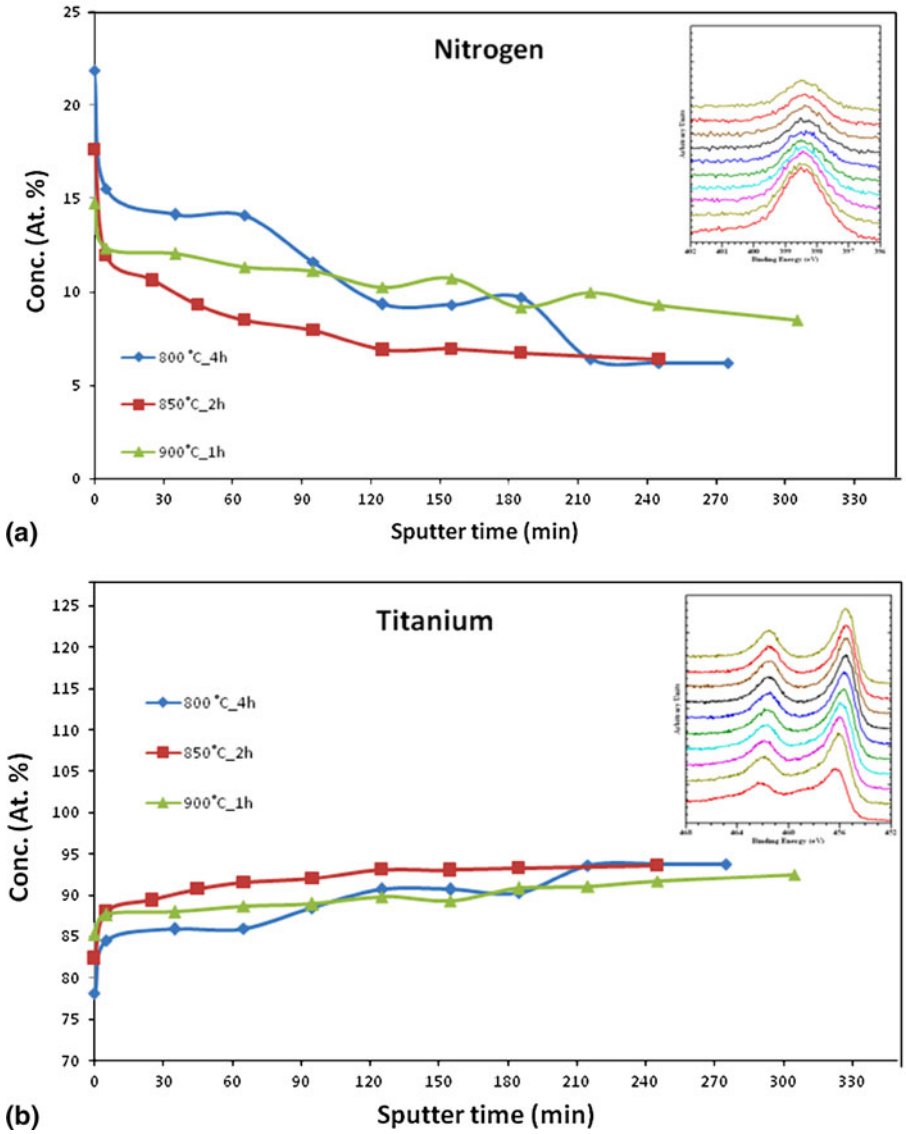

Fig. 8 Distribution of nitrogen (a) and titanium (b) in samples nitrided at different temperatures in 100% N (inset: XPS spectra of (a) N1s and (b) Ti2p core levels obtained at different depths from samples nitrided for 4 h at 800 °C)

acoustic and longitudinal acoustic (TA + LA) phonons occur in the 200-400 cm^{-1} wave number range, which correspond to nitrogen vacancies in the lattice (Ref 24). As seen in the spectra, significant intensities can be observed only after 800 °C nitriding, and at lower temperatures, the intensities of the peaks are low, especially in the 550-800 cm^{-1} wave number range. For samples treated for 8 h in 100% N, Raman peaks were observed in the wave number range of 210-220 cm^{-1}, close to that of standard nitride TA/LA peaks. In the case of samples nitrided with hydrogen dilution, the spectral features do not resemble that of TiN, and at higher wave number range of 500-800 cm^{-1}, peaks are not clear. The ratio of the TO + LO phonon peak intensities to that of TA + LA acoustic phonon intensities in TiN_x has been used as a measure of concentration of nitrogen vacancies in TiN_x. If the intensity ratio is lower than 1, then the nitrogen concentration, x, is lower than unity (Ref 25-27). From a qualitative assessment of the Raman spectra shown in Fig. 6(a) and (b), it is clear that x is less than 1 in these samples. This shows that nitrogen intake by the samples is lower than that needed for stoichiometric TiN formation.

Table 2 shows the atomic percentage of nitrogen under samples after 8 h of nitriding in 100% N at different temperatures, and Table 3 compares the nitrogen concentrations in samples nitrided for 8 h at 750 °C and 800 °C under 100% N, 80% N-20% H, and 80% N-20% Ar gas compositions. It can be observed from the above tables that significant increase in nitrogen concentration can be observed only after nitriding at greater than 750 °C, and after nitriding at 850 °C, nitrogen concentration reaches 33.7 at.%. Further, it can be seen from Table 3 that hydrogen dilution increases nitrogen concentration in the nitrided layers, whereas argon dilution leads to a nominal decrease. In stoichiometric TiN, the nitrogen concentration is 50 at.% and in Ti_2N, it is 33.3 at.%. Therefore, as deduced from Raman spectral intensities and X-ray diffraction data, the nitrogen concentration is lower than that expected from the one that is needed for TiN formation, and the EDS results shown in Table 3 support is conclusion.

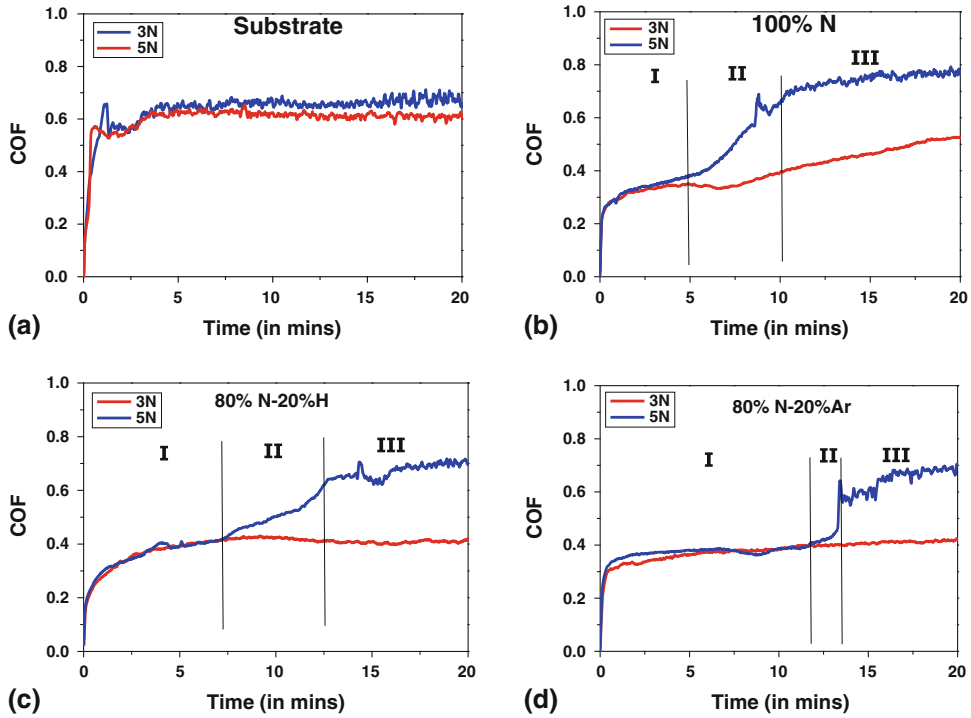

Fig. 9 COF versus time on (a) substrate and samples nitride at 800 °C for 4 h, (b) 100% N, (c) 80% N-20% H, and (d) 80% N-20% Ar

Table 4 COF and wear loss for substrate and nitrided samples

	Average COF under different loads							
	Region-I		Region-II		Region-III		Wear loss (mm^3)	
	3N	5N	3N	5N	3N	5N	3N	5N
Substrate	0.6	0.6	…	…	…	…	0.14	0.225
100% N	0.3	0.3	0.3	0.5-0.7	0.3	0.7	…	0.155
80-20% N-H	0.3	0.3	0.3	0.4-0.6	0.3	0.6	…	0.075
80-20% N-Ar	0.3	0.3	0.3	0.4-0.6	0.3	0.6	…	0.075

FESEM images of the surface morphologies of the samples nitrided at 800 °C for 8 h are shown in Fig. 7(a)-(c) for various gas compositions. It can be seen from the micrographs that in the case of samples nitrided with 100% nitrogen, the surface has ridge-like structure whereas that in argon the diluted-case the surface appears rough with nanometer-sized precipitates present on the surface. In the case of samples nitrided with hydrogen-diluted nitrogen, the surface appears smoother. This is in conformity with earlier results of surface roughness measurements, where samples nitrided with hydrogen dilution had lower surface roughness values.

Figure 8(a) and (b) shows nitrogen and titanium distribution in the samples after nitriding in 100% nitrogen at different temperatures. The insets in the figures show the Ti2p and N1s core level spectra after sputter etching for different durations. In the case of Ti2p core level spectra, oxide as well as nitride peaks are present on the surface with Ti2p3/2 core level-binding energies at 458 and 456 eV, respectively (Ref 28-30). After etching for few minutes, the oxide is removed, and only nitride is present. Further etching shifts the peak position to lower binding energy values with increasing sputtering time. In the case of N1s core level, the peak binding energy is at 398.5 eV, corresponding to nitrogen in nitride form and shifts to lower BE values with sputter etching. After nitriding for 4 h at 800 °C, the surface nitrogen concentration is about 23 at.% and decreases sharply with respect to sputtering time. After nitriding for 2 h at 850 °C the surface concentration is 17 at.% and decreases with increasing sputter depth less steeply. After nitriding at 900 °C for 1 h, the surface concentration is 15 at.%, but its decreases very slowly with increasing sputter time. These profiles show that at temperatures lower than 850 °C, the diffusion of nitrogen is low, and significant diffusion takes place only at higher temperatures. This trend in diffusion is reflected in the intake of nitrogen in the near-surface region and consequent hardness increase and its profile that could be achieved. The hardness profiles shown in Fig. 1(a) and (b) shows that hardness decreases rapidly with load and also that the hardness profile is nearly flat as shown in Fig. 2(a) and (b). Since intake of nitrogen is low, alpha titanium is observed as nitrogen is an alpha stabilizer, and Ti_2N is the predominant phase formed. Precipitates of TiN may be formed as evidenced from the low intensity of TiN peaks in the XRD. As nitrogen diffusion coefficient is low in titanium at temperatures lower than 800 °C, the nitrided layer thickness is also low.

The wear and frictional properties of the substrate and samples nitrided at different conditions were investigated in a linear reciprocating wear test. The evolutions of coefficient of friction (COF) for different loads in the linear reciprocating wear test are shown in Fig. 9(a)-(d). The average values of COF and wear loss for the Ti-15-3 substrate and nitrided samples are given in Table 4. While in the case of substrate the COF increases rapidly to a high value of 0.6 at both 3N and 5N loads, the nitrided samples behave differently. In these cases, the COF is low at 3N load, especially for the samples nitrided with diluted nitrogen; at 5N load, three regimes can be seen in the figures in the evolution of the friction coefficient. In region-I, the COF is low (0.3-0.4), and in region-III, it is close to that of substrate with a transition in region-II. The COF increases gradually in the transition region. Thus, nitriding considerably reduces the friction at low loads, and at higher loads, once the nitrided layer is removed, the COF reaches that of substrate. Dilution of nitrogen with hydrogen or argon increases duration of region-I, the low-COF region. Hydrogen dilution further provides a gradual transition to region-III.

The 3D profiles of wear tracks on the substrate and nitrided samples are shown in Fig. 10 for 3N load. In the case of substrate, the profile shows clear wear profile, from which wear loss can be estimated. For the nitrided samples, the wear profile was smoother with no clear wear profile, suggesting negligible wear. The 2D and 3D wear profiles of the wear tracks at 5N load are shown in Fig. 11(a) for the substrate and for nitrided samples in Fig. 11(b)-(d). It can be seen from the 2D and 3D profiles in Fig. 11(a) that the wear profile on the substrate has deep grooves of several microns depth, while the wear tracks on the nitrided samples appear less deep. The 2D wear profiles of the samples at higher magnification are shown in Fig. 11(a)-(d). The figs show that nitriding with dilution decreases wear, as the wear tracks appear smoother than those on the substrate and sample nitrided with 100% nitrogen. Wear loss shown in Table 4 indicates that nitriding reduces the wear loss. In the case of substrate, the wear loss nearly doubles to 0.225 mm^3 from 0.14 mm^3 for increase in load from 3N to 5N. After nitriding, the wear is negligible for 3N load. For 5N load, after nitriding with 100% N, wear loss is reduced by 50% to 0.15 mm^3, while for samples nitrided with dilution of nitrogen with H and Ar, it is further reduced to 0.07 mm^3. Thus, the appearance of deep grooves in wear tracks and the considerable wear loss at 3N load itself suggest that the wear is abrasive in nature in the case of substrate. In the case of nitrided samples, the 3D wear profile is smoother, and wear loss is negligible at 3N load. The COF is also lower during the entire duration of wear testing. At 5N load, the wear loss is lower than that of substrate, and the COF is low in region-I. This shows that the wear mechanism has changed from abrasive wear on the substrate to adhesive wear after nitriding. At higher loads, once the nitrided layer is removed, the wear mechanism changes to abrasive wear as seen from the wear profile and higher COF at the end of the wear test. Further, the transition from region-I to III is gradual in the case of samples nitrided with hydrogen dilution. Thus, nitriding with diluted nitrogen, especially with

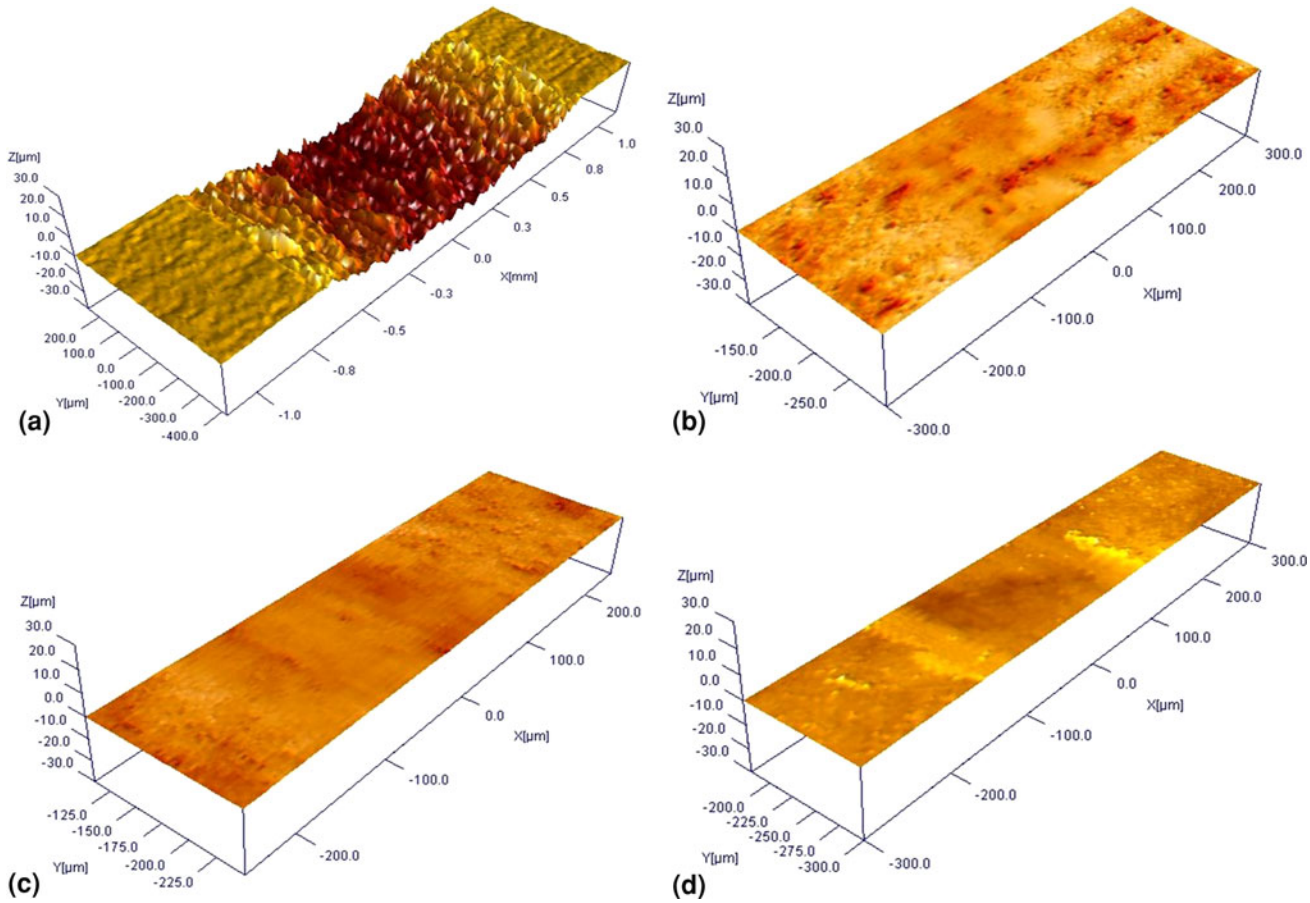

Fig. 10 Profiles of wear tracks in 3D at 3N load on (a) substrate and samples nitrided at 800 °C for 4 h, (b) 100% N, (c) 80% N-20% H, and (d) 80% N-20% Ar

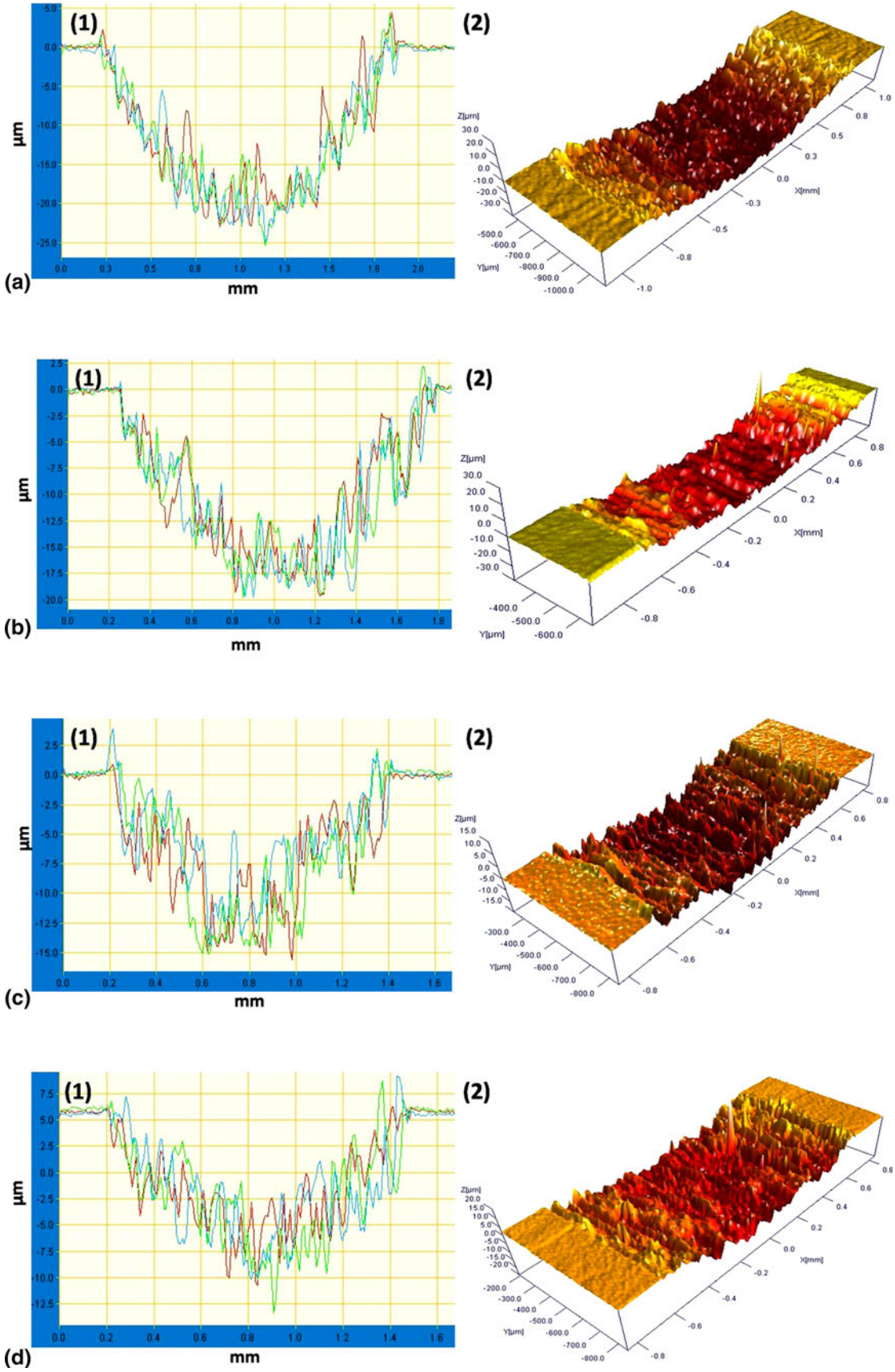

Fig. 11 (1) 2D and (2) 3D profiles of wear tracks at 5N load at high resolution on (a) substrate and samples nitrided at 800 °C for 4 h, (b) 100% N, (c) 80% N-20% H, and (d) 80% N-20% Ar

hydrogen, improves the wear behavior of the titanium alloy Ti-15-3 by reducing the COF and decreasing the wear loss.

The above results on nitrided titanium alloy Ti-15-3 show that the alloy has poor nitridability. Even though the beta transus temperature of the alloy is low, i.e., 750-770 °C, the alloy has to be heated to temperatures >800 °C for effective nitriding to take place. This implies that irrespective of beta transus temperatures, titanium alloys have to be heated to temperatures greater than 800 °C for effective nitriding. Hydrogen dilution helps in increasing the nitrogen intake as can be seen from the hardness data and EDS results. It is known that hydrogen removes the surface oxide by etching and also increases ionization of nitrogen in the plasma. The removal of the oxide barrier and the availability of more nitrogen ions and atoms due to increased ionization increase the intake of nitrogen by the sample. Even then, the nitriding kinetics is low at temperatures lower than 800 °C. With argon dilution, the sample surface is sputtered during the nitriding process, and also the partial pressure of nitrogen is lowered. While sputtering removes the oxide as well as nitrided layers, the reduced nitrogen partial pressure decreases the intake of nitrogen and helps in controlling the composition of nitrided layer. Analyses of the nitrided layers by EDS, micro Raman, and XPS show that intake of nitrogen is lower at temperatures lowers than 800 °C. The lower intake of nitrogen leads to the formation of α phase and predominantly Ti_2N formation, as seen in XRD. Depth profiling of the nitrided layers by XPS shows that diffusion of nitrogen into the interior of the sample is low. All these factors determine the hardness, the hardness profile, and the wear behavior of the nitrided samples as discussed above.

4. Conclusions

Beta titanium alloy, Ti-15V-3Cr-3Al-3Sn (Ti-15-3) was plasma nitrided in low-pressure RF plasma using nitrogen and nitrogen diluted with hydrogen and argon at temperatures less than and greater than the beta transus temperature of the material. The results show that effective nitriding of the alloy can occur only at temperatures higher than the beta transus temperature, and even then the intake of nitrogen is low. XRD shows the formation of alpha phase, and predominantly, Ti_2N. Micro Raman spectra, EDS, and XPS show that nitrogen concentration in the nitrided layer is low. Depth profiling by XPS shows that nitrogen profile in the material is shallow. This is reflected in the hardness and its profile in the nitrided layers. Wear studies show a low COF and lower wear loss for plasma-nitrided samples, especially with hydrogen dilution.

Acknowledgments

The study was carried under the 11th five-year plan projects on enhancement of knowledge base in aerospace materials project SIP-SED-05 funded by CSIR-NAL. The authors would like to thank Director, NAL for permission to publish this research; and Head, SED for constant encouragement. The authors would like to thank Mr. Siju, Mr. NT. Manikandanath, Mr. Praveen, and Mr. Muniprakash for various characterizations.

References

1. R. Boyer, G. Welsch, and E.W. Collings, *Materials Properties Handbook: Titanium Alloys*, ASM International, Materials Park, 2003
2. C. Leyens and M. Peters, *Titanium and Titanium Alloys: Fundamentals and Applications*, Wiley-VCH, Germany, 2003
3. K.G. Budinski, Tribological Properties of Titanium Alloys, *Wear*, 1992, **151**, p 203–217
4. S.M. Johns, T. Bell, M. Samandi, and G.A. Collins, Wear Resistance of Plasma Immersion Ion Implanted Ti6A14V, *Surf. Coat. Technol.*, 1996, **85**, p 7–14
5. H. Dong and T. Bell, Designer Surfaces for Titanium Components, *Ind. Lubr. Tribol.*, 1998, **50**(6), p 282–289
6. H. Dong and T. Bell, Ti-2003 Science and Technology, *Proceedings of the 10th World Conference on Titanium: Volume-II*, G. Lutjering and J. Albrecht, Eds., Wiley-VCH, Germany, 2004
7. X. Liu, P.K. Chu, and C. Ding, Surface Modification of Titanium, Titanium Alloys, and Related Materials for Biomedical Applications, *Mater. Sci. Eng. R*, 2004, **47**, p 49–121
8. X. Qiu, J.R. Conrad, R.A. Dodd, and F.J. Worzala, Plasma Source Nitrogen Ion Implantation of Ti-6Al-4V, *Metall. Trans. A*, 1990, **21A**, p 1663–1667
9. B.Y. Tang, P.K. Chu, S.Y. Wang, K.W. Chow, and X.F. Wang, Methane and Nitrogen Plasma Immersion Ion Implantation of Titanium Metal, *Surf. Coat. Technol.*, 1998, **103-104**, p 248–251
10. S.Y. Wang, P.K. Chu, B.Y. Tang, X.C. Zeng, Y.B. Chen, and X.F. Wang, Radio Frequency Plasma Nitriding and Nitrogen Plasma Immersion Ion Implantation of Ti6Al4V, *Surf. Coat. Technol.*, 1997, **93**, p 309–313
11. E.S. Metin and O.T. Inal, Microstructure and Microhardness Evaluations in Ion Nitrided Titanium, *Mater. Sci. Eng. A*, 1991, **145**, p 65–77
12. C. Lugmair, R. Kullmer, A. Gebeshuber, C. Mitterer, M. Stoiber, H. Patrovsky, and M. Adley, *Ti-2003 Science and Technology, Proceedings of the 10th world conference on Titanium: Volume-II*, G. Lutjering and J. Albrecht, Eds., Wiley-VCH, Germany, 2004
13. U. Huchel and S. Stramke, *Ti-2003 Science and Technology, Proceedings of the 10th world conference on Titanium: Volume-II*, G. Lutjering and J. Albrecht, Eds., Wiley-VCH, Germany, 2004
14. K.N. Strafford and J.M. Towell, The Interaction of Titanium and Titanium Alloys with Nitrogen at Elevated Temperatures. I. The Kinetics and Mechanism of the Titanium-Nitrogen Reaction, *Oxid. Met.*, 1976, **10**, p 41–67
15. K.N. Strafford and J.M. Towell, The Interaction of Titanium and Titanium Alloys with Nitrogen at Elevated Temperatures. II. The Nitridation Behaviour of Alloys Containing 5 wt.% Percent of Aluminium and Chromium, *Oxid. Met.*, 1976, **10**, p 69–84
16. E. Metin and O.T. Inal, Kinetics of Layer Growth and Multiphase Diffusion in Ion Nitrided Titanium, *Metall. Trans. A*, 1989, **20A**, p 1819–1832
17. N.R. McDonald and G.R. Wallwork, The Reaction of Nitrogen with Titanium Between 800 and 1200°C, *Oxid. Met.*, 1970, **2-3**, p 263–283
18. A. Zhecheva, W. Sha, S. Malinov, and A. Long, Enhancing the Microstructure and Properties of Titanium Alloys Through Nitriding and Other Surface Engineering Methods, *Surf. Coat. Technol.*, 2005, **200**, p 2192–2220
19. A. Zhecheva, S. Malinov, and W. Sha, Titanium Alloys After Surface Gas Nitriding, *Surf. Coat. Technol.*, 2006, **201**, p 247–2467
20. W. Sha and S. Malinov, *Titanium Alloys: Modelling of Microstructure, Properties and Applications*, Woodhead Publishing Ltd., Cambridge, 2009
21. Prateek Kumar, P. Dilli Babu, L. Mohan, C. Anandan, and V.K. William Grips, Wear and Corrosion Behavior of Zr-Doped DLC on Ti-13Zr-13Nb Biomedical Alloy, *J. Mater. Eng. Perform.*, 2012, doi: 10.1007/s11665-012-0230-3
22. S.L.R. da Silva, L.O. Kerber, L. Amaral, and C.A. dos Santos, X-Ray Diffraction Measurements of Plasma Nitrided Ti6Al4V, *Surf. Coat. Technol.*, 1999, **116-119**, p 342–346
23. F.M. El-Hossary, N.Z. Negm, S.M. Khalil, and M. Raaif, Surface Modification of Titanium by Radio Frequency Plasma Nitriding, *Thin Solid films*, 2006, **497**, p 196–202
24. M.A.Z. Vasconcellos, R. Hinrichs, C.S. Javorsky, G. Giuriatti, and J.A.T. Borges da Costa, Micro-Raman Characterization of Plasma Nitrided Ti6Al4V-ELI, *Surf. Coat. Technol.*, 2007, **202**, p 275–279

25. C.P. Constable, J. Yarwood, and W.D. Munz, Raman Microscopic Studies of PVD Hard Coatings, *Surf. Coat. Technol.*, 1999, **116-119**, p 155–159
26. R. Chowdhury, R.D. Vispute, K. Jagannadham, and J. Narayan, Characteristics of Titanium Nitride Films Grown by Pulsed Laser Deposition, *J. Mater. Res*, 1996, **11**(6), p 1458
27. Y.H. Cheng, B.K. Tay, S.P. Lau, H. Kupfer, and F. Richter, Substrate Bias Dependence of Raman Spectra for TiN Films Deposited by Filtered Cathodic Vacuum Arc, *J Appl. Phys.*, 2002, **92**(4), p 1845
28. N.C. Saha and H.G. Tompkins, Titanium Nitride Oxidation Chemistry: An X-Ray Photoelectron Spectroscopy Study, *J. Appl. Phys.*, 1992, **72**, p 3072
29. A. Gicquel, N. Laidani, P. Saillard, and J. Amouroux, Plasma and Nitrides: Application to the Nitriding of Titanium, *Pure Appl. Chem.*, 1990, **62-69**, p 1743–1750
30. E. Galvanetto, F.P. Galliano, F. Borgioli, U. Bardi, and A. Lavacchi, XRD and XPS Study on Reactive Plasma Sprayed Ti-Ti Nitride Coatings, *Thin Solid Films*, 2001, **384**, p 223–229